UPDATED FLAT-FIELDS OF ONC-T/HAYABUSA2 BASED ON CLOSE ENCOUNTER WITH RYUGU.

E. Tatsumi[1], S. Kameda[2], K. Moroi[2], M. Ishida[2], T. Kouyama[3], R. Honda[4], T. Morota[5], M. Yamada[6], Y. Yokota[7], N. Sakatani[7], H. Suzuki[8], C. Honda[9], K. Yoshioka[1], Y. Cho[1], M. Matsuoka[7], M. Hayakawa[7], K. Ogawa[10], H. Sawada[7], S. Sugita[1], [1]Univ. of Tokyo (eri@eps.s.u-tokyo.ac.jp), [2]Rikkyo Univ., [3]National Inst. of Adv. Industrial Sci. and Tech., [4]Kochi Univ., [5]Nagoya Univ., [6]Chiba Inst. of Tech., [7]ISAS/JAXA, [8]Meiji Univ., [9]Univ. of Aizu., [10]Kobe Univ.

Introduction: Hayabusa2 arrived at the Cb-type asteroid Ryugu on 27 June 2018. The telescopic Optical Navigation Camera (ONC-T) is a multi-band visible camera onboard Hayabusa2, which provides visible spectrophotometry and enables geomorphologic study of the target asteroid. We conducted a series of onboard calibrations during the cruise phase [1,2], which included electromagnet interference noise, dark current, linearity, stray lights, and detector sensitivities. The flat-field corrections were tested using star images, and it was found that the flat-fields do not completely remove the non-uniformity in the detector response within the field-of-view (FOV). This is mainly due to the stray light and temperature differences between the on-ground calibration measured with the integrating sphere [3] and in-flight conditions. Because the object is very dark and relatively uniform, the quality of the flat-fields need to be improved. For example, to detect the 0.7-μm band absorption associated with phyllosilicates at a ~3-4% level, requires less than 1% of flatness in the spatial sensitivity deviation.

ONC-T is equipped with 7 band-pass filters; ul: 0.40 μm, b: 0.48 μm, v: 0.55 μm, Na: 0.59 μm, w: 0.70 μm, x: 0.86 μm, p: 0.95 μm. We found that the flat-field for ul-band is heavily contaminated by the roundabout stray lights [1]. Moreover, the NIR wavelengths, such as the x- and p-bands, have etalon fringing patterns and the UV wavelengths, such as the ul- and b-bands, have scratch patterns in the flat-fields which create interference reflection patterns on the CCD (Fig. 1). It was confirmed with on-ground tests that these patterns change with CCD temperature due to slight changes in CCD dimensions. The preflight flat-fields were obtained at room temperature, while the onboard temperature is typically -30 ˚C. Thus, we decided to improve the flat-field characterization using in-flight images of Ryugu.

Method and Dataset: During the MASCOT lander operations on 3 and 4 October 2018, the spacecraft hovered at altitude of ~3 km. The images obtained during these operations filled the image frame with the surface of Ryugu. 24 sets of 7-band images were acquired. We began by choosing a reference flat-field with a minimum of patterns due to the anti-reflection coat, which is usually optimized for the

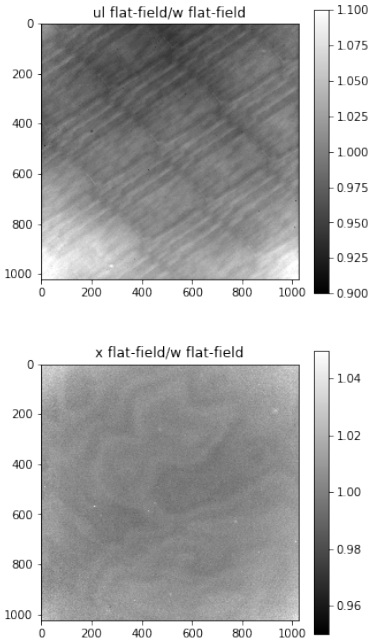

Fig. 1 Old flat-field patterns for ul-band (top) and x-band (bottom).

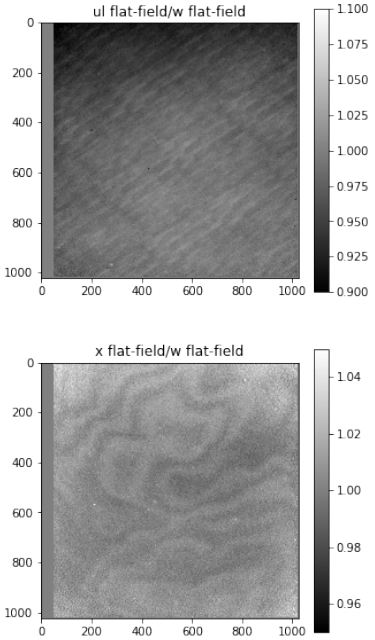

Fig. 2 New flat-field patterns for ul-band (top) and x-band (bottom).

center of visible wavelength region. The idea here was to modify the reference flat-field and obtain updated flat-fields of other filters by comparisons. The important assumption here is that the surface of Ryugu is very homogeneous and there is only very small spectral variation across its surface. The step-by-step procedure for generating the new flat-fields is described below:

1. The reference filter images are co-aligned with the images taken in the other filters due to the small difference in the observed time.
2. Because we assume that the ratio of a reference filter image to another filter image is essentially the ratio of the flat-fields, we can define a temporal flat-field as:
   n-band new temporal flat-field = (reference filter image)*(reference flat-field)/(n-band image),
   where n is the filter name (ul, b, v, w, Na, x, p).
3. Each image set yields one set of 7-band flat-fields.
4. We created updated flat-fields by averaging the 24 temporal flat-fields from each image set, within each band. Some 'outlier' pixels were removed from the averaging due to the presence of shadows in the images from boulders on the surface. Removal of outlier pixels resulted in averaging ~16 images for each pixel.

Evaluation: The new flat-fields (Fig. 2) were evaluated using image sets on the same region acquired with slightly different geometries (sets of 20181003_151510 and 20181003_225509). We co-aligned the images and assessed the ratio between two aligned images to which the updated flat-fields were applied. Ideally, the two images should be identical even though the same surface area was captured in difference parts of FOV. The ratio image is binned by 128x128 pixels, excluding the outliers due to shadows of boulders. An example of the ratio of the binned images is shown in Fig. 3. We assessed the flatness using the 3-sigma of 5x7 bins, common coverage (Table 1). This assessment shows the improvement in flatness especially in ul-band. The new flat-field corrections yield less than 1% deviation across the FOV.

Table 1 Flatness scores for old and new flat-fields. The score was assessed by the 3-sigma among 5x7 boxes with 128x128 pixels.

	Old flat-fields	New flat-field
ul	3.2%	0.5%
b	0.8%	0.4%
v	0.4%	-
Na	0.8%	0.4%
w	0.9%	0.4%
x	0.9%	0.6%
p	1.2%	0.6%

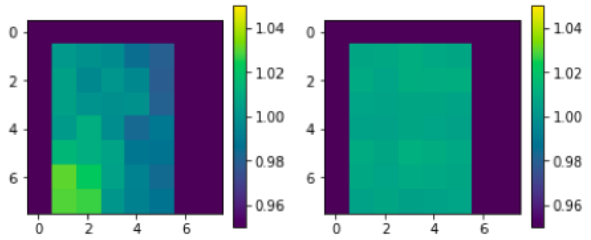

Fig. 3 Ratio between two aligned images binned in 128 x 128 pixels. Old flat-fields (left) and new flat-fields (right) were applied. One which new flat-fields are applied show better flatness.

Applications: The spectral slope is calculated using the previous and new flat-fields (Fig. 4, top). The previous one shows a redder slope at the edge of FOV, while the new one shows more uniform color variations. Next, we measured the 0.7-μm band absorption using the new flat-fields (Fig. 4, bottom). Before the update, the 0.7-μm band absorption map was dominated by the patterns in the flat-fields, especially in x-band, while the pattern is no longer present in the map. The 0.7-μm band absorption map shows homogeneous properties over the surface, with no clear detection of an absorption in the 0.7-μm band.

Acknowledgement: This study is supported by JSPS core-to-core program "International Network of Planetary Sciences" and JSPS KAKENHI (18H01264).

References: [1] Suzuki, H., et al. (2018) *Icarus*, 300, 341-359. [2] Tatsumi, E., et al. (2019) *Icarus*, submitted, arxiv.org/abs/1810.11065. [3] Kameda, S., et al. (2017) *SSR, 208*, 17-31.

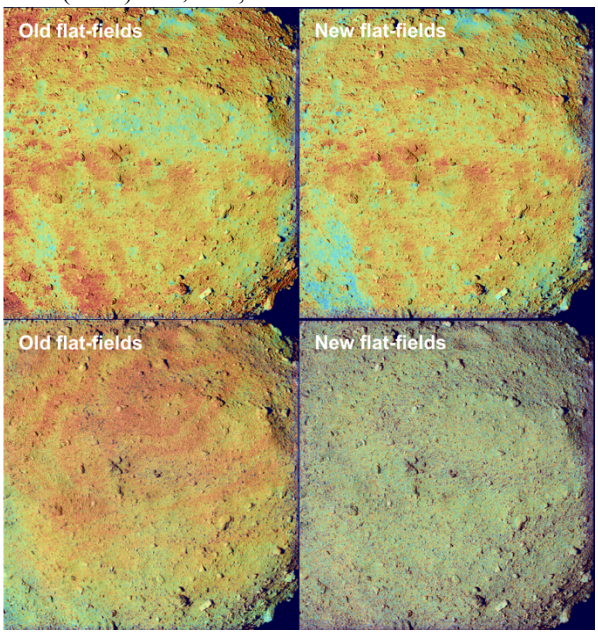

Fig. 4 Spectral feature maps using old and new flat-fields: spectral slope (top) and 0.7-μm band absorption (bottom).